

Supplemental material

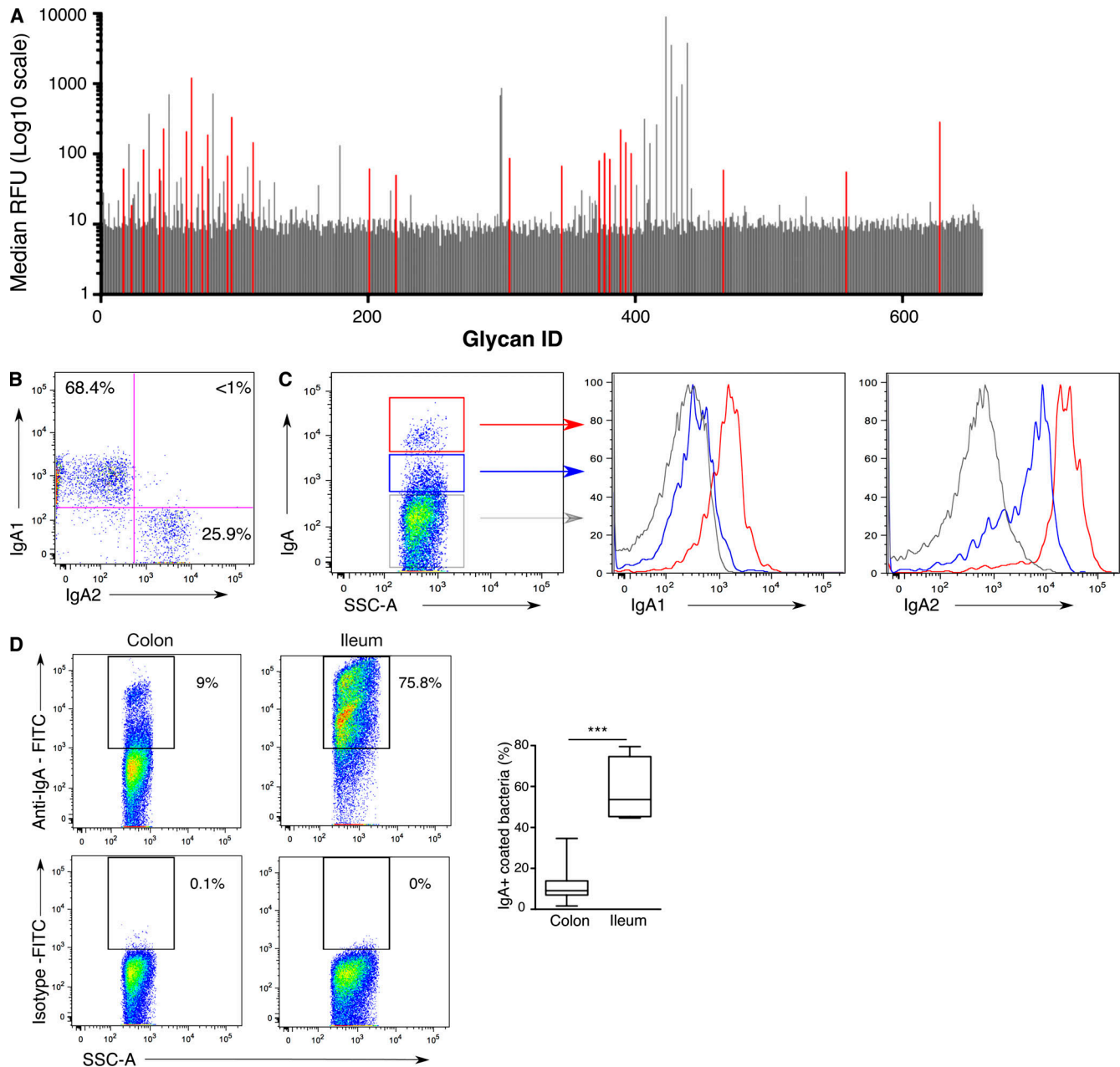


Figure S1. Gut bacteria segregate into IgA^{bright} and IgA^{low} fractions in healthy humans. Related to Figs. 1 and 2. **(A)** The secretory component binds a modest range of carbohydrates. Glycan reactivity with the secretory component was assessed using glycan microarray technology (660 structures). Representative median RFUs are shown. Glycans specifically recognized by secretory component are colored in red. **(B)** Anti-IgA1 and anti-IgA2 antibodies do not cross-react. Flow cytometry analysis of IgA1 and IgA2 expression on peripheral B cells from a healthy donor. **(C)** IgA-coated bacteria split into IgA^{bright} and IgA^{low} fractions depending on IgA1 and IgA2 coating. Representative flow cytometry analysis of IgA1 and IgA2 coating in IgA^{bright}-coated bacteria (red lines), IgA^{low}-coated bacteria (blue lines), and IgA-unbound bacteria (gray lines). **(D)** Representative flow cytometric analysis of colon and ileum microbiota (left and central panels, respectively) with anti-IgA FITC or isotype-matched control antibody, as indicated. Numbers indicate percentage of positive cells. Data are cumulative from three independent experiments. Boxes extend from the 25th to the 75th percentiles. Error bars represent minimum and maximum values. P values were defined using the Mann-Whitney test. ***, P < 0.001. SSC-A, side scatter area. Quantification of IgA-coated bacteria in stool (n = 20) and ileum (n = 5).

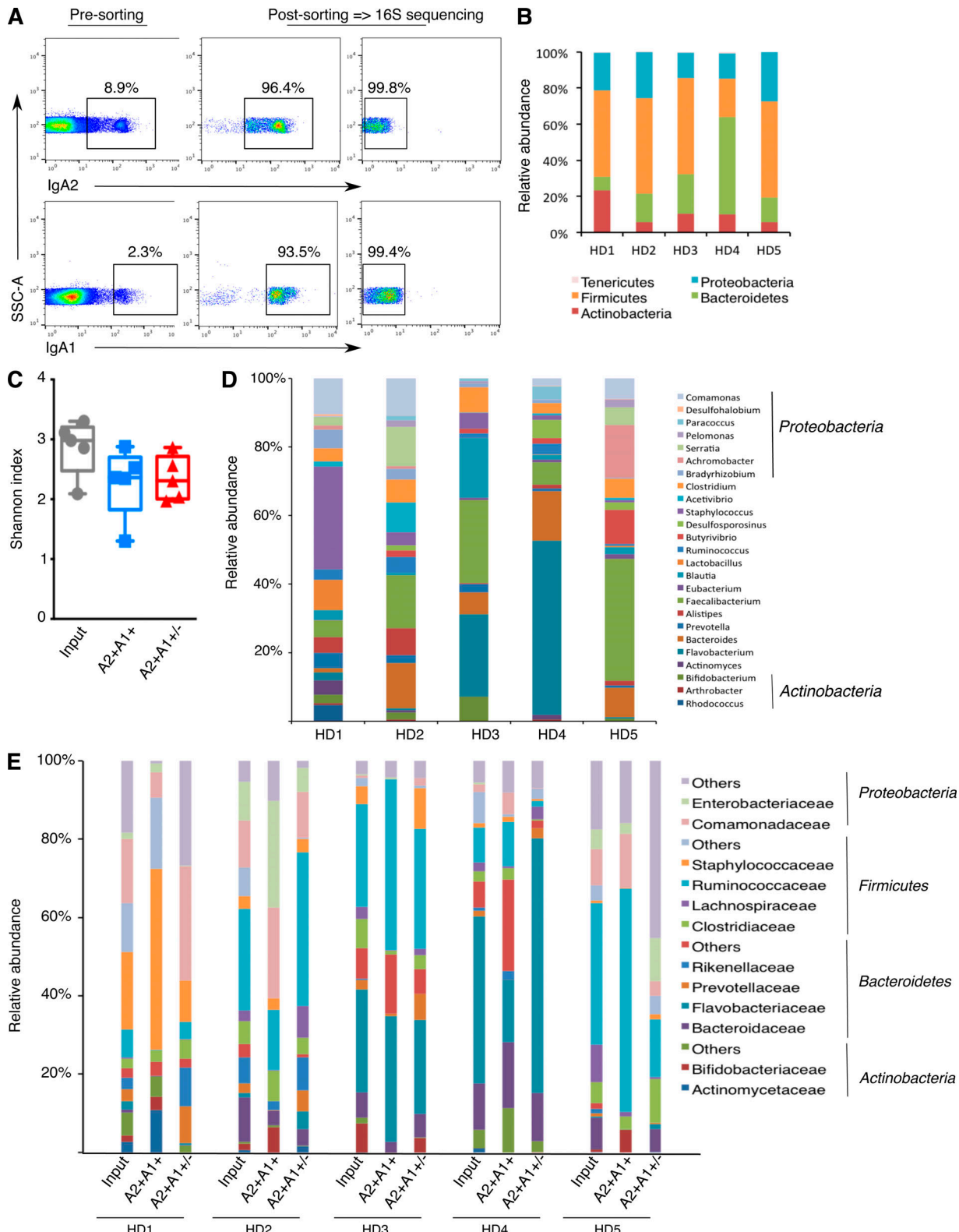


Figure S2. IgA1⁺IgA2⁻ and IgA2⁺-sorted fractions show distinct compositions within the same donor and between donors. Related to Fig. 4. **(A)** Sorting strategy of IgA1- and IgA2-coated bacteria (representative of five independent experiments). SSC-A, side scatter area. **(B)** Relative composition of phyla in fecal samples (input). Each column corresponds to one healthy donor (HD) sample out of five analysed (HD1 to HD5, as indicated). **(C)** Genera diversity of input, IgA1⁺, and IgA2⁺ fractions calculated using the Shannon index. Boxes extend from the 25th to the 75th percentiles. Error bars represent minimum and maximum values. **(D)** Relative composition of genera in fecal samples (input). Each column corresponds to one sample. The 25 most abundant genera are shown. **(E)** Relative abundance of families in input and sorted fractions from five healthy donors. The top 16 most abundant families are shown.

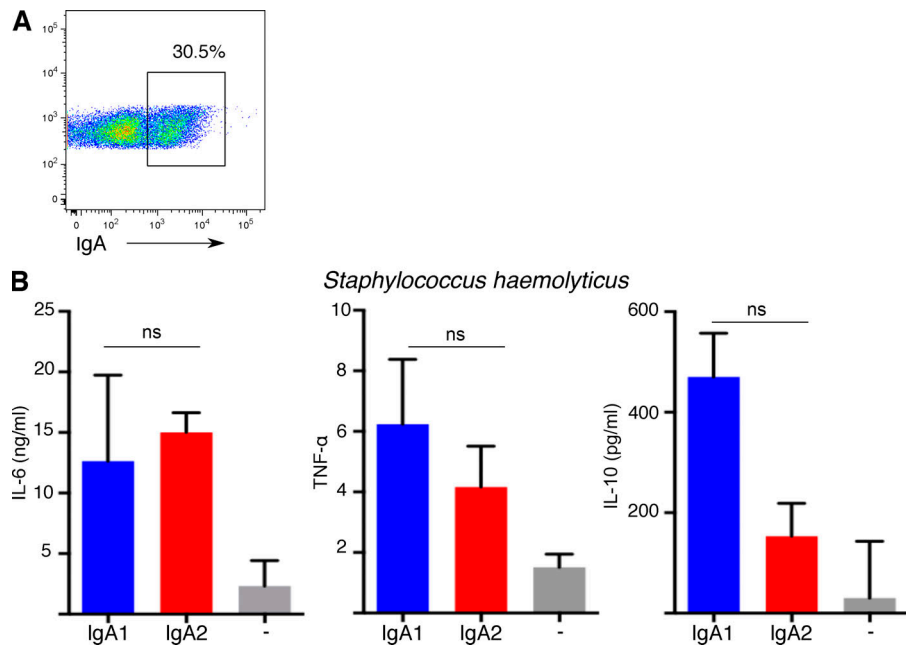


Figure S3. IgA1- and IgA2-coated bacteria promote cytokine production by macrophages. (A) One out of three representative flow cytometric analyses of human gut microbiota purified from an IgA-deficient donor incubated with breast milk IgA and subsequently with anti-IgA FITC (three independent experiments). Numbers indicate percentage of positive cells. **(B)** Cytokine levels measured using Simoa technology in supernatants of macrophages incubated for 24 h with heat-killed *S. haemolyticus* opsonized with IgA1 (blue) or IgA2 (red) or without IgA (gray). The Mann-Whitney test was used to calculate P values; ns, not significant ($n = 3$ healthy donors, two independent measurements). Error bars indicate maximum values.

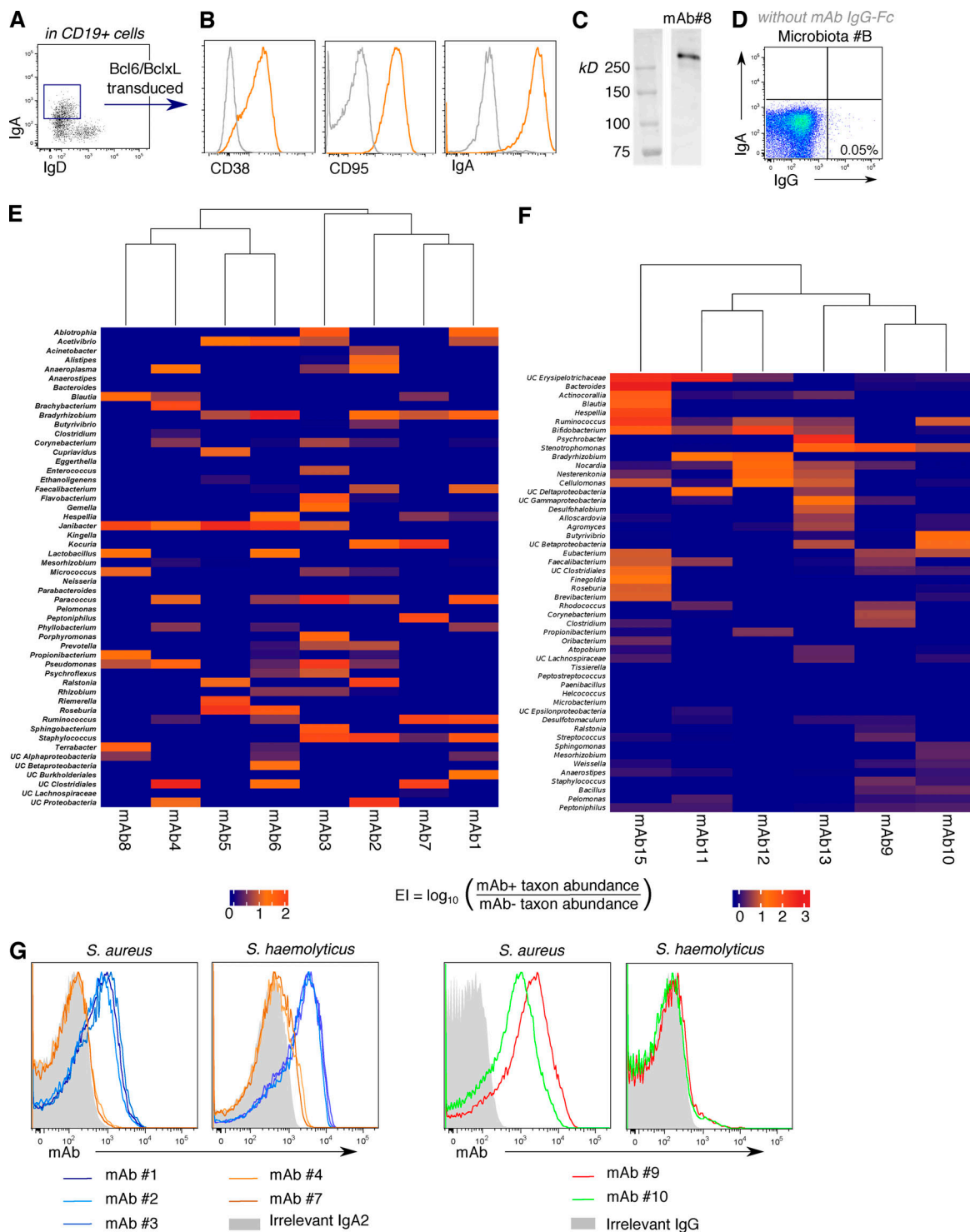


Figure S4. Human monoclonal IgA bind a broad but nevertheless private pattern of commensals. Related to Fig. 4. **(A)** Flow cytometric sorting of intestinal IgA⁺ memory B cells (defined as CD19⁺, cell surface IgA⁺ IgD⁻). Sort gate among CD19⁺ B cells is shown. Doublets and dead cells were excluded before CD19 gating, CD19⁺ cells were gated among CD45⁺ cells (not shown). Representative images from three independent sorts are shown. **(B)** Transduced B cells exhibited a stable germinal center-like phenotype and maintained IgA expression. Transduced B cells were surface-labeled with anti-CD38, anti-CD95, or anti-IgA (orange lines) or appropriate isotype antibody controls (gray dotted lines). Representative images of eight monoclonal B cell lines, evaluated in three independent experiments, are shown. **(C)** Monoclonal B cell lines produced dimeric IgA. Representative immunoblotting showing high molecular weight dimeric mAb in nonreducing conditions for mAb 8. Representative image of eight mAbs and two independent experiments are shown. **(D)** Representative flow cytometric plot of microbiota B stained with anti-IgG Alexa Fluor 647 and anti-IgA FITC. The same experiment was repeated twice. **(E)** Heatmap diagram of EI of the 50 most frequent genera from microbiota A. Hierarchical clustering grouped mAb⁺ fractions and genera. **(F)** Heatmap diagram of EI of the 50 most frequent genera from microbiota B. Hierarchical clustering grouped mAb⁺ fractions and genera. **(G)** Flow cytometric analysis of mAb or negative control (mAb⁻ supernatant [left] or irrelevant IgG [right, anti-TNF α IgG1]) staining of pure bacterial strains (two independent experiments).

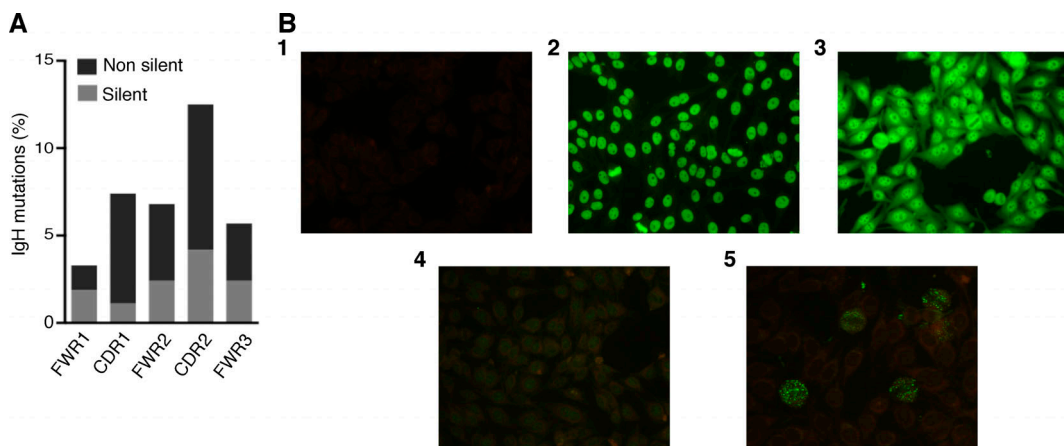


Figure S5. Self-reactivity and glycan reactivity of antigen-selected secretory IgA. **(A)** Median frequency of nonsilent (black) and silent (gray) somatic mutations in CDRs and VH FWRs in mAb *IGH* genes ($n = 16$ mAbs, four independent experiments). **(B)** Self-reactivity was tested by IFA with HEp-2000 cells: (1) negative control; (2) positive control: autoimmune human serum containing anti-DNA; (3) purified IgA from fecal water (20 μ g/ml); (4) negative staining representative of 15 nonreactive mAbs; and (5) mAb 4. Representative images of three independent experiments are shown.

Tables S1–S3 are provided online as separate Excel files. Table S1 lists Ig gene analysis of dimeric monoclonal antibodies. Table S2 contains the demographic data of human samples. Table S3 lists primers for Ig and 16s rDNA gene sequence analysis.